J|A|C|S
ARTICLES
Published on Web 05/23/2002

Chemistry of a Novel Family of Tridentate Alkoxy Tin(II) Clusters

Timothy J. Boyle,* Judith M. Segall, Todd M. Alam, Mark A. Rodriguez, and Jessica M. Santana

Contribution from the Sandia National Laboratories, Advanced Materials Laboratory, 1001 University Boulevard SE, Albuquerque, New Mexico, 87106

Received February 14, 2002

Abstract: The chemical interconversions observed for a novel family of trihydroxymethyl ethane (THME-H_3) ligated Sn(II) compounds have been determined using single-crystal X-ray and ^{119}Sn NMR experiments. (μ-THME)$_2$Sn$_3$ (**1**) was isolated from the reaction of 3 equiv of [Sn(NR$_2$)$_2$]$_2$ (R = SiMe$_3$) with 4 equiv of THME as a unique trinuclear species capped above and below the plane of Sn atoms by two THME ligands. Upon reaction with "Sn(NR$_2$)$_2$", compound **1** rearranged to yield another novel molecule [(μ-THME)Sn$_2$-(NR$_2$)]$_2$ (**2**). Compound **2** could also be formed directly from the stoichiometric mixture of THME-H_3 and [Sn(NR$_2$)$_2$]$_2$. Further studies revealed that **1** would also rearrange in the presence of Sn(OR)$_2$ to form [(μ-THME)Sn$_2$(μ-OR)]$_2$ [OR = OMe (**3**), OCH$_2$Me (**4**), OCH$_2$CH(Me)CH$_2$CH$_3$ (**5**), OCH$_2$CMe$_3$ (**6**, ONep), OC$_6$H$_5$ (**7,** not structurally characterized), OC$_6$H$_4$Me-3 (**8**), OC$_6$H$_4$Me-2 (**9**), OC$_6$H$_3$(Me)$_2$-2,6 (**10**), OC$_6$H$_3$(CHMe$_2$)$_2$-2,6 (**11**). Additionally, **3**−**11** could by synthesized from the reaction of **2** and the appropriate H−OR. ^{119}Sn solution NMR studies of **2**−**11**, in THF-d_8, indicate that an equilibrium between the parent complex and its disassociation products (**1** and the free parent Sn alkoxy or amide precursor) exists at room temperature. This is a likely reason behind the ease of interconversion observed for **1**. The generality of this exchange was further verified through the reaction of **1** with [Ti(μ-ONep)(ONep)$_3$]$_2$, which led to the isolation of (μ-ONep)$_2$Sn$_3$(μ-THME)$_2$Ti(ONep)$_2$ (**12**). For **12**, the solid-state structure was maintained in solution with no indication of an equilibrium.

Introduction

Tin oxide (SnO_x) ceramic materials have demonstrated utility in such varied applications as glass coatings,[1,2] flat panel displays,[3] reversible thermoelectric converters,[4] solar cells,[5,6] gas sensors (NO_x, CO_x, HOR, CH_4),[1,3,7−16] LED instruments,[17,18] optoelectronic devices,[3,19,20] phosphors,[21] and anodes of Li^+ batteries.[22−24] Metal alkoxides (M(OR)$_x$) are excellent precursors to ceramic materials due to their high solubility, high volatility, low decomposition temperatures, ease of modification, and commercial availability.[25−29] The hydrolysis and condensation rates of the M(OR)$_x$ are often altered through the introduction of modifying ligands to optimize the properties of the final material. Since the characteristics of the metal alkoxide precursors greatly affect the properties of the final ceramic material,[25−30] it is critical to know the structural aspects of these compounds,

* To whom correspondence should be sent. E-mail: tjboyle@Sandia.gov.

(1) Koh, S. K.; Jung, H. J.; Song, S. K.; Choi, W. K.; Choi, D.; Jeon, J. S. U.S. Patent US598990, 1999.
(2) Clough, T. J.; Gosvenor, V. L.; Pinsky, N. U.S. Patent US5756192, 1998.
(3) Martel, A.; Caballero-Briones, F.; Fandino, J.; Castro-Rodriguez, R.; Bartolo-Perez, P.; Zapata-Navarro, A.; Zapata-Torres, M.; Pena, J. L. *Surf. Coat. Technol.* **1999**, *122*, 136.
(4) Yater, J. C.; Yater, J. A.; Yater, J. E. U.S. Patent US5889287, 1999.
(5) Veluchamy, P.; Tsuji, M.; Nishio, T.; Aramoto, T.; Higuchi, H.; Kumazawa, S.; Shibutani, S.; Nakajima, J.; Arita, T.; Ohyama, H. *Sol. Energy Mater. Sol. Cells* **2001**, *67* (MAR), 179.
(6) Amin, N.; Isaka, T.; Yamada, A.; Konagai, M. *Sol. Energy Mater. Sol. Cells* **2001**, *67* (MAR), 195.
(7) Abbas, M. N.; Moustafa, G. A.; Gopel, T. V. *Anal. Chim. Acta* **2001**, *4331*, 181.
(8) Chaudhary, B. A.; Mulla, I. S.; Vijayamohanan, K.; Hegde, S. G.; Srinivas, D. *J. Phys. Chem. B* **2001**, *105*, 2565.
(9) Hellegouarc'h, F.; Arefi-Khonsari, F.; Planade, R.; Amouroux, J. *Sens. Actuators, B* **2001**, *73*, 27.
(10) Gregory, O. J.; Luo, Q. *Sens. Actuators, A* **2001**, *88*, 234.
(11) Tarabek, J.; Wolter, M.; Rapta, P.; Plieth, W.; Maumy, M.; Dunsch, L. *Macromol. Symp.* **2001**, *164*, 219.
(12) Yoshimi, Y.; Ohdira, R.; Iiyama, C.; Sakai, K. *Sens. Actuators, B* **2001**, *73*, 49.
(13) Koh, S. K.; Jung, H. J.; Song, S. K.; Choi, W. K.; Choi, D.; Jeon, J. S. U.S. Patent US6059937, 2000.
(14) Chou, J. C.; Chung, W.-Y.; Hsiung, S.-K.; Sun, T.-P.; Liao, H.-K. U.S. Patent US6218208, 2001.
(15) Chang, S.-C. U.S. Patent US4169369, 1979.
(16) Sangaletti, L.; Depero, L. E.; Dieguez, A.; Marca, G.; Morante, J. R.; Romano-Rodriguez, A.; Sberveglieri, G. *Sens. Acutators, B* **1997**, *44*, 268.
(17) Ishikawa, H.; Lippey, B.; Kobayashi, T.; Oshima, Y.; Mitsuhashi, S.; Yamashita, M.; Honjo, Y.; Kaneko, K. U.S. Patent US6284382, 2001.
(18) Forrest, S.; Thompson, M. E.; Burrows, P. E.; Sapochak, L. S.; McCarty, D. M. U.S. Patents US5757026, 1998; US5721160, 1998; and US5707745, 1998.
(19) Gamard, A.; Jousseaume, B.; Toupance, T.; Campet, G. *Inorg. Chem.* **1999**, *38*, 4671.
(20) Jimenez, V. M.; Espinos, J. P.; Caballero, A.; Contreras, L.; Fernandez, A.; Justo, A.; Gonzalez-Elipe, A. R. *Thin Solid Films* **1999**, *353*, 113.
(21) Chadha, S. S.; Alwan, J. J. U.S. Patent US5695809, 1997.
(22) Nam, S. C.; Yoon, Y. S.; Cho, W. I.; Cho, B. W.; Chun, H. S.; Yun, K. S. *Electr. Commun.* **2001**, *3*, 6.
(23) Nam, S. C.; Yoon, Y. S.; Cho, W. I.; Cho, B. W.; Chun, H. S.; Yun, K. S. *J. Electrochem. Soc.* **2001**, *148* (MAR), A220.
(24) Mohamedi, M.; Lee, S. J.; Takahashi, D.; Nishizawa, M.; Itoh, T.; Uchida, I. *Electrochem. Acta* **2001**, *46*, 1161.
(25) Hubert-Pfalzgraf, L. G. *New J. Chem.* **1987**, *11*, 663.
(26) Chandler, C. D.; Roger, C.; Hampden-Smith, M. J. *Chem. Rev.* **1993**, *93*, 1205.
(27) Bradley, D. C. *Chem. Rev.* **1989**, *89*, 1317.
(28) Bradley, D. C.; Mehrotra, R. C.; Gaur, D. P. *Metal Alkoxides*; Academic Press: New York, 1978.
(29) Bradley, D. C.; Mehrotra, R. C.; Rothwell, I. P.; Singh, A. *Alkoxo and Aryloxo Derivatives of Metals*; Academic Press: San Diego, CA, 2001.

10.1021/ja0202309 CCC: $22.00

both in solution and in the solid sate, to fully exploit them. On the basis of the diverse applications of cassiterite thin films, it is surprising that only a few simple tin alkoxide ($Sn(OR)_x$) species have been crystallography characterized, including $[Sn(OR)_4(HOR)]_2$ (OR = $OCHMe_2$[31,32] or $OCH_2C(H)Me_2$[33]), $[Sn(OCH_2Ph)_4(HN(CH_3)_2)]_2$,[34] $[Sn(OC(CH_3)_2\text{-}C_6H_4)_2]_2$,[34] $Sn(OCMe_3)_4$,[31] $[Sn(OCMe_3)_2]_2$,[35,36] $Sn(OCH(CF_3)_2)_4 \cdot HNMe_2$,[37] and $Sn(OCH(CF_3)_2)_2 \cdot HNMe_2$.[38] Additional Sn(II) and Sn(IV) aryloxide species have also been characterized as mono- or dinuclear complexes based on the steric bulk of the ring substituent.[34] This small number of $Sn(OR)_x$ precursors, with limited geometrical arrangements, greatly limits the properties of final ceramic materials that can be obtained.

We have been investigating the structural aspects of metal alkoxide compounds using mono-, di-, and tridentate ligands.[39−48] Recently, through the introduction of the monodentate neopentoxide (ONep = OCH_2CMe_3) ligand, we isolated the unusual polymeric Sn(II) species $[Sn(\mu\text{-ONep})_2]_\infty$.[45,47] By using bidentate carboxylic acids, several Sn(II) oxo, alkoxy carboxylate structures have been characterized; however, due to esterification, control over the structure of the resultant complexes has been limited.[47] This was not the case for the tridentate ligated $Sn(OR)_x$ system, wherein the introduction of the tridentate ligand tris(hydroxymethyl)ethane ($H_3CC(CH_2OH)_3$ = THME-H_3) ligand was used as a means to generate a family of structurally controlled molecules (Scheme 1).

The syntheses of THME-modified $Sn(OR)_2$ compounds led to the isolation and characterization of a unique Sn(II) compound,[49] (μ-THME)$_2Sn_3$ (**1a**−**e**). Further studies on chemical modification of this compound led to the characterization of $[(\mu\text{-THME})Sn_2(N(SiMe_3)_2)]_2$ (**2**) and $[(\mu\text{-THME})Sn_2(\mu\text{-OR})]_2$ [OR = OMe (**3**), OCH_2Me (OEt, **4**), $OCH(Me)CH_2CH_3$ (OBu^{Me}, **5**), ONep (**6**), and OC_6H_5 (OPh, **7**, not structurally characterized), OC_6H_4Me-3 (mMP, **8**), OC_6H_4Me-2 (oMP, **9**), $OC_6H_3Me_2$-2,6 (DMP, **10**), and $OC_6H_3(CHMe_2)_2$-2,6 (DIP, **11**)]. To explore the generality of this structural incorporation, the early transition metal alkoxide, $[Ti(\mu\text{-ONep})(ONep)_3]_2$,[40] was reacted with **1** and the unique mixed metal species to yield (μ-ONep)$_2Sn_3(\mu\text{-THME})_2Ti(ONep)_2$ (**12**). The synthesis of this unique family of compounds, **1**−**12**, the various interexchanges these compounds undergo, and exploitable physical properties are presented.

Experimental Section

All compounds described were handled with rigorous exclusion of air and water, using standard Schlenk line and glovebox techniques. All solvents [hexanes (hex), toluene (tol), tetrahydrofuran (THF), pyridine (py), dioxane (diox)], as well as, H-OMe and H-OEt, were freshly distilled from the appropriate drying agent,[50] immediately prior to use. The following chemicals were used as received (Aldrich): $SnCl_2$, $LiNR_2$ (R = Me, $SiMe_3$), THME-H_3, H-OBu^{Me}, H-ONep, H-oMP, H-DMP, H-DIP, and H-DBP. The appropriate "$Sn(NR_2)_2$" was synthesized from the reaction of $SnCl_2$ and 2 equiv of $LiNR_2$ in THF.[51] The $Sn(OR)_2$ precursors were synthesized from $Sn(NMe_2)_2$ and ∼2 equiv of the appropriate HOR (HOR = H-OMe, H-OEt, HONep, H-OBu^{Me}, H-OPh, H-mMP, H-oMP, H-DMP, H-DIP). $[Ti(\mu\text{-ONep})(ONep)_3]_2$ was prepared as reported in the literature.[40] For additional information concerning the analytical data collection methodologies see the Supplemental Information.

(μ-THME)$_2Sn_3$ (1). THME-H_3 (7.23 g, 64.4 mmol) was added to a solution of $[Sn(N(SiMe_3)_2]_2$ (20.0 g, 96.6 mmol) in hex (30 mL) with stirring, which formed a white precipitate over time. The reaction was stirred for an additional 12 h and then warmed (60 °C) for 1 h to ensure completeness of the reaction. The volatile material was removed by rotary evaporation to yield an off-white powder. This material was washed with a minimal amount of hex and dried again. Crystals were grown from hot solutions of **1** in hex (**1a**), tol (**1b**), THF (**1c**), py (**1d**), and diox (**1e**) which were either concentrated and allowed to sit at glovebox temperatures or cooled to −35 °C until crystals formed. Yield 15.4 g (81.2%, from hexanes). ^{119}Sn (149.1 MHz, THF-d_8) δ −330. Anal. Calcd for $C_6H_{18}Sn_3$: 20.34, C; 3.07, H. Found: 20.42, C; 3.03, H. FTIR (KBr, cm^{-1}) 951(m), 2923(m), 2900(m), 2833(m), 2787(m), 2731(m), 2672(m), 1458(m), 1397(s), 1130(s), 1043(s), 595(s), 450-(s).

[(THME)Sn$_2$(NR$_2$)]$_2$ (2). To a vial of $[Sn(N((SiMe_3)_2)_2]_2$ (1.00 g, 1.14 mmol) dissolved in THF (∼7 mL) was added THME-H_3 (0.137 g, 1.14 mmol) with stirring. The reaction was heated to a boil, allowed to cool with stirring over 12 h, heated to a boil again, and allowed to cool to room temperature. The volatile material was removed by rotary evaporation to yield a pale yellow powder. This material was washed with hexanes, heated in THF, and allowed to cool to room temperature whereupon crystals were isolated. Crystalline yield 0.250 g (22.0%). ^{119}Sn (149.1 MHz, THF-d_8) δ +12, −331, −451. Anal. Calcd for $C_{22}H_{54}N_2O_6Si_4Sn_4$: 54.60, C; 5.29, H; 2.72, N. Found: 37.50, C; 7.96, H; 6.24, N. FTIR (KBr, cm^{-1}) 2950(s), 1459(m), 1400(m), 1245(m), 1130(m), 1052(s), 941(m), 835(m), 670(m), 601(m), 454(w).

General Syntheses of [(μ-THME)$_2$Sn$_2$(μ-OR)]$_2$ (3−11). To a solution of **1** in tol (∼7 mL) was added the appropriate $Sn(OR)_2$ with stirring, which resulted in a clear solution. After 12 h, the reaction was warmed for 1 h, the volume of the reaction mixture was drastically reduced by rotary evaporation, and the mixture was cooled to −35 °C or it was allowed to set loosely sealed at glovebox temperature until crystals formed. Full synthesis and analytical data for **3**−**11** are listed in the Supporting Information. For the representative compounds shown in this paper, the full details are listed below.

(30) Boyle, T. J.; Tyner, R. P.; Alam, T. M.; Scott, B. L.; Ziller, J. W.; Potter, B. G. J. *J. Am. Chem. Soc.* **1999**, *121*, 12104.
(31) Hampden-Smith, M. J.; Wark, T. A.; Rheingold, A.; Huffman, J. C. *Can. J. Chem.* **1991**, *69*, 121.
(32) Reuter, H.; Kremser, M. *Z. Anorg. Allg. Chem.* **1991**, *598/599*, 259.
(33) Chandler, C. D.; Caruso, J.; Hampden-Smith, M. J.; Rheingold, A. L. *Polyhedron* **1995**, *14*, 2491.
(34) Smith, G. D.; Visciglio, V. M.; Fanwich, P. E.; Rothwell, I. P. *Organometallics* **1992**, *11*, 1064.
(35) Fjeldberg, T.; Hitchcock, P. B.; Lappert, M. F.; Smith, S. J.; Thorne, A. J. *Chem. Commun.* **1985**, 939.
(36) Veith, M.; Hobein, P.; Rosler, R. *Z. Naturforsch., Teil B* **1989**, *44*, 1067.
(37) Suh, S.; Hoffman, D. M.; Atagi, L. M.; Smith, D. C.; Liu, J.-R.; Chu, W.-K. *Chem. Mater.* **1997**, *9*, 730.
(38) Suh, S.; Hofman, D. M. *Inorg. Chem.* **1996**, *35*, 6164.
(39) Boyle, T. J.; Schwartz, R. W.; Doedens, R. J.; Ziller, J. W. *Inorg. Chem.* **1995**, *34*, 1110.
(40) Boyle, T. J.; Alam, T. M.; Mechenbeir, E. R.; Scott, B.; Ziller, J. W. *Inorg. Chem.* **1997**, *36*, 3293.
(41) Boyle, T. J.; Alam, T. M.; Dimos, D.; Moore, G. J.; Buchheit, C. D.; Al-Shareef, H. N.; Mechenbier, E. R.; Bear, B. R. *Chem. Mater.* **1997**, *9*, 3187.
(42) Boyle, T. J.; Pedrotty, D. M.; Scott, B.; Ziller, J. W. *Polyhedron* **1997**, *17*, 1959.
(43) Boyle, T. J.; Alam, T. M.; Tafoya, C. J.; Scott, B. L. *Inorg. Chem.* **1998**, *37*, 5588.
(44) Boyle, T. J.; Gallegos, J. J., III; Pedrotty, D. M.; Mechenbier, E. R.; Scott, B. L. *J. Coord. Chem.* **1999**, *47*, 155.
(45) Boyle, T. J.; Alam, T. M.; Rodriguez, M. A.; Zechmann, C. A. *Inorg. Chem.* **2002**, *41*, 2574.
(46) Boyle, T. J.; Alam, T. M.; Peter, K. P.; Rodriguez, M. A. *Inorg. Chem.* **2002**, *40*, 6281.
(47) Boyle, T. J.; Jackson, N.; Miller, J.; Segall, J. M.; Alam, T. M.; Zechmann, C. A.; Rodriguez, M. A. *Abstracts of Papers*; 221st National Meeting of the American Chemical Society April 1, 2001; American Chemical Society: Washington, DC, 2001; Abstract U748.
(48) Zechmann, C. A.; Boyle, T. J.; Pedrotty, D. M.; Alam, T. M.; Lang, D. P.; Scott, B. L. *Inorg. Chem.* **2001**, *40*, 2177.
(49) Boyle, Timothy J. U.S. Patent US6307078, 2001.
(50) Perrin, D. D.; Armarego, W. L. F. *Purification of Laboratory Chemicals*, 3rd ed.; Pergamon Press: New York, 1988.
(51) Harris, D. H.; Lappert, M. F. *Chem. Commun.* **1974**, 895.

Scheme 1. Reaction Pathway for THME-Modified $Sn(OR)_2$

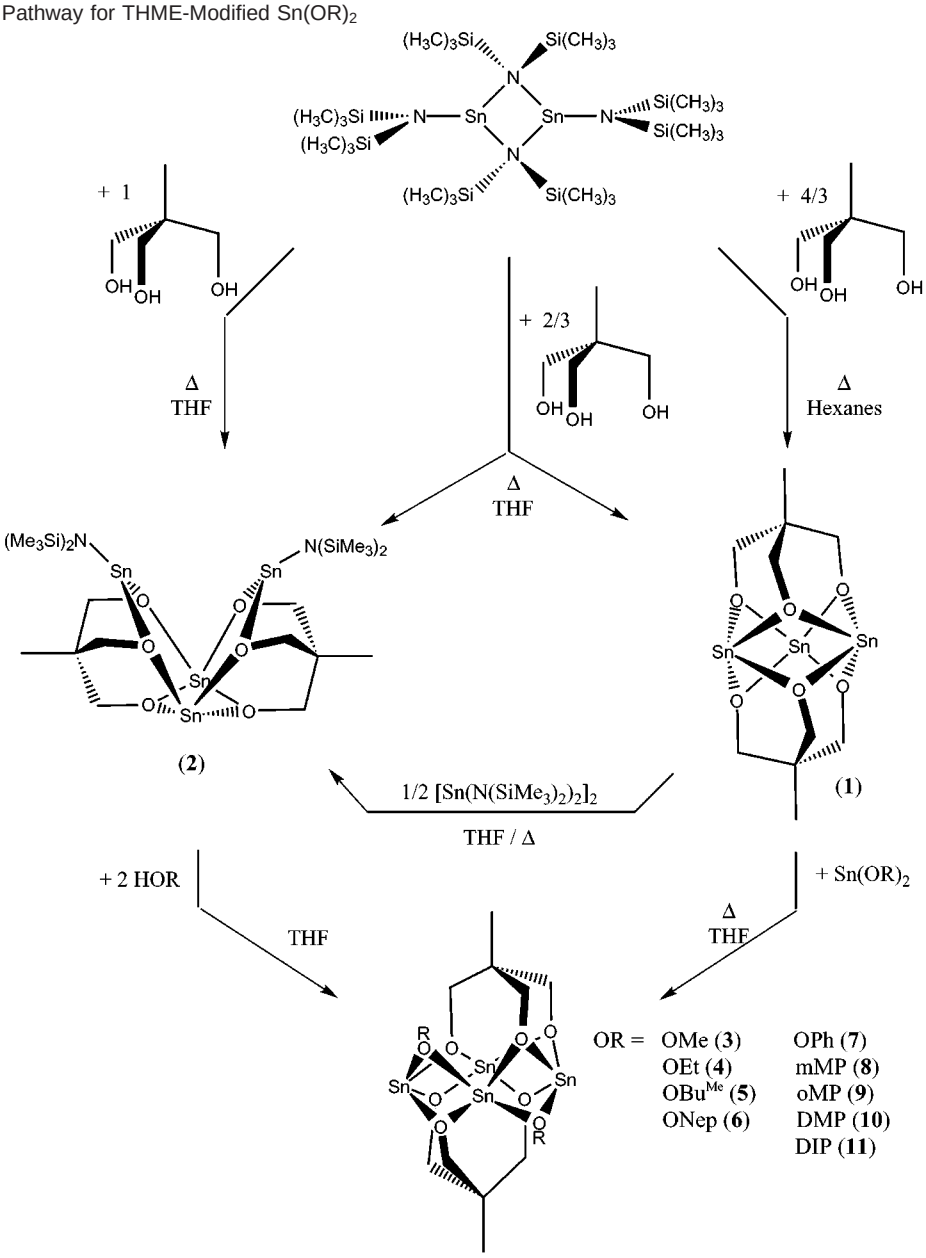

[(μ-THME)Sn_2(μ-ONep)]$_2$ (6). $Sn(ONep)_2$ (0.50 g, 1.7 mmol) and **1** (1.0 g, 1.7 mmol) in THF (∼5 mL) were used. Crystalline yield 1.3 g (84%). Anal. Calcd for $C_{20}H_{40}O_8Sn_4$: 27.20, C; 4.53, H. Found: 27.45, C; 4.43, H. ^{119}Sn (149.1 MHz, THF-d_8) δ −330 (0.66 Sn), −366 (1.0 Sn), −377 (2.0 Sn), −387 (1.0 Sn). FTIR (KBr, cm^{-1}) 2949(m), 2923(sh,m), 2829(m), 2798(m), 2705(m), 2675(m), 1474(sh,m) 1458-(m), 1406(sh, m), 1356(m), 1120(s), 1038(s), 1012(sh,s), 907(w), 608-(m), 557(sh,m), 445(m), 432(sh,m).

[(μ-THME)Sn_2(μ-DIP)]$_2$ (11). $Sn(DIP)_2$ (0.80, 1.7 mmol) and **1** (1.0 g, 1.7 mmol) in THF (∼5 mL) were used. Crystalline yield 0.89 g (55%). FTIR (KBr, cm^{-1}) 2957(m), 1459(m), 1431(m), 1382(m), 1361-(w,sh), 1313(m), 1258(m), 1179(m), 1118(m), 1041(s), 932(sh,w), 825-(m), 799(w), 755(w), 732(w), 489(w). Anal. Calcd for $C_{34}H_{52}O_8Sn_4$: 38.40, C; 4.93, H. Found: 38.86, C; 5.21, H. ^{119}Sn (149.1 MHz, THF-d_8) δ −208, −309, −339, −390, −403.

(μ-ONep)$_2$$Sn_3$(μ-THME)$_2$Ti(ONep)$_2$ (12). To a solution of **1** (1.0 g, 1.7 mmol) in tol (∼7 mL) was added $[Ti(ONep)_4]_2$ (0.67 g, 0.85 mmol) with stirring, which resulted in a clear solution. After 12 h, the reaction was warmed for 1 h, the volume of the reaction mixture was drastically reduced by rotary evaporation, and the mixture was allowed to set loosely sealed at glovebox temperature until crystals formed. Crystalline yield 0.92 g (55%). FT-IR (KBr, cm^{-1}) 2951(s), 2864(s), 2825(s), 2745(m), 2681(m), 1287(w), 1260(w), 1561(w), 1544(w), 1509(w), 1476(m), 1460(m), 1450(w), 1439(w), 1403(m), 1390(m), 1361(m), 1260(m),1215(m), 1128(s), 1109(s,sh), 1054(s), 1020(s), 932-(w), 899(w), 809(w), 751(w), 671(m), 658(s), 620(m), 583(m), 513-(s), 465(s), 438(w). Anal. Calcd for $C_{30}H_{62}O_{10}Sn_3Ti$: 36.52, C; 6.33, H. Found: 36.83, C; 6.12, H. ^{119}Sn (149.1 MHz, THF-d_8) δ −358 (1 Sn), −403 (2 Sn).

X-ray Crystal Structures.[52] Tables 1− 3 list the data collection parameters for **1a**−**e**, **2**−**6**, and **8**−**12**, respectively. All crystals were mounted onto a thin glass fiber from a pool of Fluorolube and placed immediately under a liquid N_2 stream on a Bruker AXS diffractometer. Structural solutions were performed by using the following software: SMART Version 5.054, SAINT+ 6.02 (7/13/99), SHELXTL 5.1 (10/29/98), XSHELL 4.1 (11/08/2000), and SADABS within the SAINT+ package.[52] Each structure was solved by using direct methods, yielding

(52) The listed versions of SAINT, SMART, XSHELL, and SADABS Software from Bruker Analytical X-ray Systems Inc., 6300 Enterprise Lane, Madison, WI 53719, were used in this analysis.

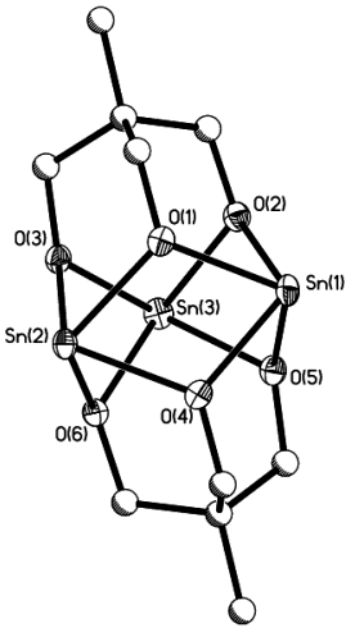

Figure 1. Thermal ellipsoid plot of $(THME)_2Sn_3$ (**1**). Thermal ellipsoid plots are drawn at the 30% level.

the Sn, O, and some of the C atoms, with subsequent Fourier synthesis yielding the remaining C atom positions. The hydrogen atoms were fixed in positions of ideal geometry and refined within the XSHELL software.[52] The final refinement of each compound included anisotropic thermal parameters on all non-hydrogen atoms. See the appropriate table or Supporting Information for additional details.

Results and Discussion

As was noted for $[(\mu\text{-THME})Ti_2(OPr^i)_5]_2$,[39] $[(\mu\text{-THME})Zr_2(OPr^i)_5]_2$,[39] and $[(\mu\text{-THME})Nb(OEt)_2]_2$,[41] the introduction of the tridentate THME ligand reduces the number of accessible terminal alkoxides which garners greater control over the condensation and hydrolysis (i.e., cross-linking) behavior of metal alkoxides. While a number of cationic and mixed halide THME ligated species for a variety of systems have been reported,[53−62] before this work there was an absence of information concerning THME-modified $Sn(OR)_x$. The reaction pathways developed for this novel family of compounds[49] (**1**−**11**) are illustrated in Scheme 1 with the details of the synthesis and characterization of these compounds presented below.

Synthesis. Initial synthetic strategies focused on generating the fully Sn-substituted THME complex; however, with a 3:1 Sn:THME stoichiometry, the temperature of the reaction mixture dictated the final product formed. When the reaction mixture was not heated, a unique, fully Sn-substituted THME ligand was isolated as $(\mu\text{-THME})_2Sn_3$ (**1**), shown in Figure 1. The yields and purity of **1** were greatly improved when hexanes and the appropriate 3:2 stoichiometry was used (eq 1). Compound

$$3\ Sn(NR_2)_2\ +\ 2\ THME\text{-}H_3 \xrightarrow{THF} (\mu\text{-THME})_2Sn_3\ +\ 6\ H\text{-}NR_2 \qquad (1)$$

1 was found to be soluble in (**a**) hex, (**b**) tol, (**c**) THF, (**d**) py, or (**e**) diox and X-ray quality crystals were isolated from each but with different unit cell dimensions and number of formula units per unit cell. The elemental analyses of the bulk powder of **1** isolated from the initial hexanes wash, and prior to crystallization, were in agreement with the solid-state crystal structure.

Compound **1** was found to be relatively air/water stable as determined by no change in the FTIR spectrum of a sample of **1** that had been exposed to atmospheric conditions for several hours. Investigation of the thermal properties of **1** by DSC revealed a melt occurred at ∼227 °C with a complete loss of material at 353 °C ($\Delta H = -165$ J/g), which is indicative of sublimation. TGA/DTA analysis of **1** revealed that this compound was stable up to ∼170 °C under an O_2 atmosphere but at higher temperatures an ∼5% weight *increase* accompanied by an exotherm in the DTA was recorded. The melting point of **1** was found to be ∼200 °C. These characteristics imply that **1** may be useful as a metalloorganic chemical vapor deposition (MOCVD) precursor.

When the original 3:1 Sn:THME reaction mixture was heated, $[(\mu\text{-THME})Sn_2(NR_2)]_2$ (**2**) was isolated and is shown in Figure 2. Improved yields were obtained for a heated 2:1 reaction mixture. Interestingly, it was also discovered that compound **2** could be synthesized from a heated mixture of **1** and $[Sn(N(SiMe_3)_2)_2]_2$ or "$Mg(N(SiMe_3)_2)_2$", as verified by single-crystal X-ray and ^{119}Sn NMR studies. Attempts to use smaller, less sterically demanding amides (i.e., $Sn(NMe_2)_2$) did not yield analogues to **2**, instead **1** was isolated. Elemental analyses of the bulk powder and the presence of NR_2 and THME stretches in the FTIR spectrum of **2** were consistent with the ligands present in the crystal structure.

The ease with which the central core of **1** was rearranged with $M(NR_2)_2$ suggested that modifications, such as $Sn(OR)_2$ (eq 2) would be possible. The alcohols used were selected to

$$(\mu\text{-THME})_2Sn_3\ +\ Sn(OR)_2 \xrightarrow{THF} (\mu\text{-THME})_2Sn_4(\mu\text{-OR})_2 \qquad (2)$$

study the effect of steric bulk on the overall structure. Independent of the steric bulk of the alcohol, **1** rearranges to incorporate the $Sn(OR)_2$ in what appears to be a side-on-addition, forming a tetranuclear species, $[(\mu\text{-THME})Sn_2(\mu\text{-OR})]_2$ where OR = OMe (**3**), OEt (**4**), OBu^{Me} (**5**), ONep (**6**), OPh (**7**), mMP (**8**), oMP (**9**), DMP (**10**), and DIP (**11**). The thermal ellipsoid plots of the alkoxide (**6**) and aryloxide (**11**) representatives are shown in Figures 3 and 4, respectively. While well-formed crystals of **7** could be grown from toluene and other solvents, the solid-state structure could not be established by single-crystal X-ray diffraction. Therefore, the mMP ligand was selected as a model to the OPh, since it has no steric bulk in the *ortho* position, as with the OPh, but offered a methyl group on the ring to alter the crystallization behavior. The structure solved for the mMP derivative, **8**, was consistent with the other compounds and based on the similarity of the steric bulk of the *ortho* position of the ring implies that the OPh also adopts a similar structure. Attempts to go beyond the steric bulk of the

(53) Chen, Q.; Zubieta, J. *Coord. Chem. Rev.* **1992**, 107.
(54) Mckee, V.; Wilkins, C. J. *J. Chem. Soc., Dalton Trans.* **1987**, 523.
(55) Hegetschweiler, K.; Schmalle, H.; Streit, H. M.; Schneider, W. *Inorg. Chem.* **1990**, *29*, 3625.
(56) Sillanp, R.; Leskel, M.; Hiltunen, L. *Acta Crystallogr.* **1982**, *B38*, 1591.
(57) Chang, Y.; Chen, Q.; Khan, M. I.; Salta, J.; Zubieta, J. *J. Chem Soc., Chem. Commun.* **1993**, 1872.
(58) Chen, Q.; Goshorn, D. P.; Scholes, C. P.; Tan, X.; Zubieta, J. *J. Am. Chem. Soc.* **1992**, *114*, 10058.
(59) Wilson, A. J.; Robinson, W. T.; Wilkins, C. J. *Acta Crystallogr.* **1983**, *C39*, 54.
(60) Cornia, A.; Gatteschi, D.; Hegetschweiler, K.; HausherrPrimo, L.; Gramlich, V. *Inorg. Chem.* **1996**, *35*, 4414.
(61) Crans, D. C.; Jiang, F.; Chen, J.; Anderson, O. P.; Miller, M. M. *Inorg. Chem.* **1997**, *36*, 1038.
(62) Jiang, F. L.; Anderson, O. P.; Miller, S. M.; Chen, J.; MahroofTahir, M.; Crans, D. C. *Inorg. Chem.* **1998**, *37*, 5439.

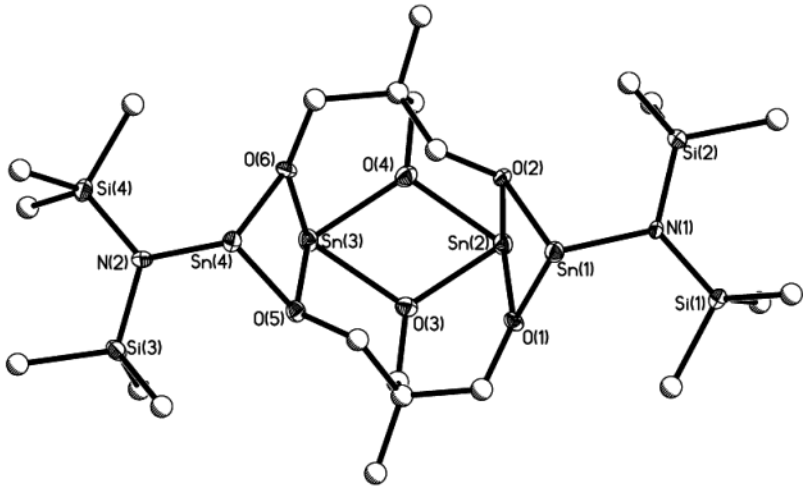

Figure 2. Thermal ellipsoid plot of $[(THME)Sn_2(NR_2)]_2$, (**2**). Thermal ellipsoid plots are drawn at the 30% level.

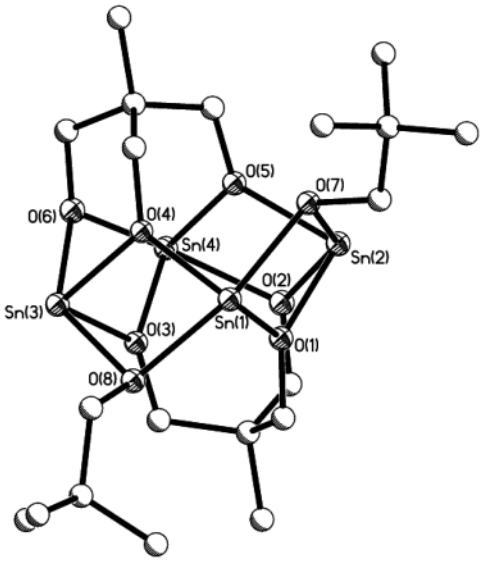

Figure 3. Thermal ellipsoid plot of $[(\mu\text{-}THME)Sn_2(OCH_2CMe_3)]_2$, (**6**). Thermal ellipsoid plotsare drawn at the 30% level.

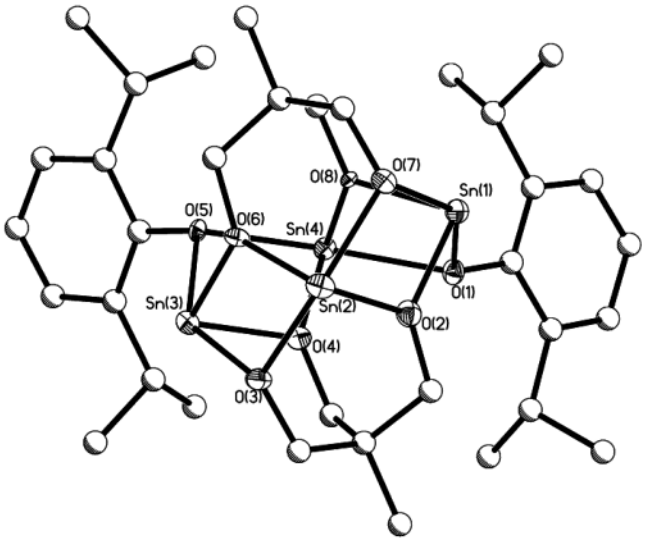

Figure 4. Thermal ellipsoid plot of $[(\mu\text{-}THME)Sn_2(OC_6H_3(CHMe_2)_2\text{-}2,6)]_2$, (**11**). Thermal ellipsoid plots are drawn at the 30% level.

bisisopropyl substituent in the 2,6 ring of **11** by using 2,6-bis-(dibutyl)phenoxide yielded only insoluble materials which could not be redissolved in a variety of solvents at elevated temperatures. This implies a change in structure but due to its low solubility, crystallographic analyses of these compounds were precluded.

Compounds **3**−**11** were found to be soluble in hexanes, toluene, THF, and py. Elemental analyses of the crystals of these compound were in agreement with the solid-state structures. The IR spectra of **3**−**11** revealed similar M−O regions;[28] however, the pendant hydrocarbon chains of the various modifiers dominated the spectra of the individual components. Compounds **3**−**11** could also be synthesized form the reaction of **2** and the respective HOR. These reactions were run on small scale so that the yields were not optimized; however, the conversions were verified by ^{119}Sn NMR analyses.

To explore the generality of the substitution of the core of **1** by metal alkoxides, we chose to investigate if the previously characterized early transition metal alkoxide $[Ti(\mu\text{-}ONep)(ONep)_3]_2$[40] would also substitute as noted for the main group $Sn(OR)_2$. Under similar conditions as noted for **3**−**11**, $[Ti(\mu\text{-}ONep)(ONep)_3]_2$[40] was reacted with **1**. The product isolated was identified as $(\mu\text{-}ONep)_2Sn_3(\mu\text{-}THME)_2Ti(ONep)_2$ (**12**) and is shown in Figure 5. Elemental analysis was consistent with the

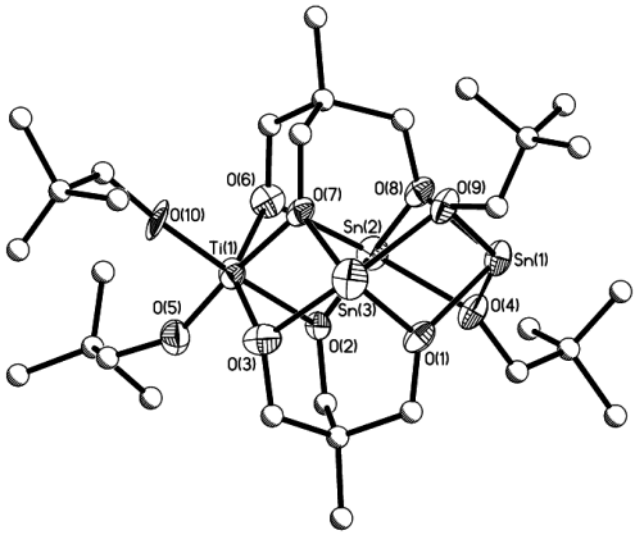

Figure 5. Thermal ellipsoid plot of $(\mu\text{-}ONep)_2Sn_3(\mu\text{-}THME)_2Ti(ONep)_2$, (**12**). Thermal ellipsoid plots are drawn at the 30% level.

Table 1. Data Collection Parameters for **1a**−**e**

	1a·hex	**1b**	**1c**·THF	**1d**·py	**1e**·diox
chemical formula	$C_{56}H_{100}O_{30}Sn_{15}$	$C_{80}H_{144}O_{48}Sn_{24}$	$C_{24}H_{44}O_{13}Sn_6$	$C_{35}H_{59}NO_{18}Sn_9$	$C_{24}H_{44}O_{14}Sn_6$
formula weight	3033.70	4722.51	1252.73	1850.04	1268.73
temp (K)	168(2)	168(2)	168(2)	168(2)	168(2)
space group	*C*2/*c*	*P*2(1)2(1)2(1)	*Pbca*	*Pnma*	*C*2/*c*
	monoclinic	orthorhombic	orthorhombic	orthorhombic	monoclinic
a (Å)	23.508(3)	21.4033(14)	12.3788(19)	22.278(4)	30.379(4)
b (Å)	12.1330(14)	24.3825(15)	22.642(3)	10.0634(16)	10.4956(15)
c (Å)	31.393(14)	24.4347(15)	25.337(4)	23.648(4)	12.4140(18)
β (deg)	109.602(2)				113.638(2)
V (Å^3)	8435.0(16)	12751.6(14)	7101.5(19)	5301.7(15)	3626.1(9)
Z	4	4	8	4	4
D_{calcd} (Mg/m^3)	2.389	2.460	2.343	2.318	2.324
μ, (Mo Kα) (mm^{-1})	4.426	4.680	4.212	4.228	4.128
*R*1[a] (%)	3.49	4.33	2.05	2.34	1.78
*wR*2[b] (%)	7.27	7.52	4.38	5.38	4.34
*R*1[a] (all data, %)	5.73	6.95	3.06	3.22	2.07
*wR*2[b] (all data, %)	7.84	8.01	4.66	5.70	4.43

[a] $R1 = \Sigma ||F_o| - |F_c||/\Sigma|F_o| \times 100$. [b] $wR2 = [\Sigma w(F_o^2 - F_c^2)^2/\Sigma(w|F_o|^2)^2]^{1/2} \times 100$.

Table 2. Data Collection Parameters for **2**−**6**

	2	**3**	**4**	**5**	**6**
chemical formula	$C_{22}H_{54}N_2O_6Si_4Sn_4$	$C_{12}H_{24}O_8Sn_4$	$C_{14}H_{28}O_8Sn_4$	$C_{20}H_{40}O_8Sn_4$	$C_{20}H_{40}O_8Sn_4$
formula weight	1029.79	771.07	799.12	883.28	883.28
temp (K)	168(2)	168(2)	168(2)	168(2)	168(2)
space group	*P*2(1)	*P*2(1)/*c*	$P\bar{1}$	*P*2(1)/*c*	$P\bar{1}$
	monoclinic	monoclinic	triclinic	monoclinic	triclinic
a (Å)	6.834(3)	14.226(3)	8.845(3)	15.051(2)	11.0984(16)
b (Å)	17.680(7)	9.1780(18)	10.630(3)	12.1069(18)	11.9361(17)
c (Å)	15.981(6)	15.553(3)	12.957(4)	15.607(2)	12.1199(17)
α (deg)			98.746(5)		109.963(2)
β (deg)	101.050(5)	95.867(3)	101.834(5)	92.027(3)	100.248(2)
γ (deg)			106.563(5)		99.461(2)
V (Å^3)	1895.1913)	2019.9(7)	1113.8(6)	2842.2(7)	1440.3(4)
Z	2	4	2	4	2
D_{calcd} (Mg/m^3)	1.805	2.536	2.383	2.064	2.037
μ, (Mo Kα) (mm^{-1})	2.765	4.922	4.467	3.512	3.465
*R*1[a] (%)	3.95	2.32	3.43	2.67	3.19
*wR*2[b] (%)	8.90	5.33	8.93	6.06	8.12
*R*1[a] (all data, %)	4.49	2.98	4.06	3.12	4.37
*wR*2[b] (all data, %)	9.21	5.54	9.36	6.25	8.86

[a] $R1 = \Sigma||F_o| - |F_c||/\Sigma|F_o| \times 100$. [b] $wR2 = [\Sigma w(F_o^2 - F_c^2)^2/\Sigma(w|F_o|^2)^2]^{1/2} \times 100$.

solid-state structure. The FTIR spectrum of **12** was similar to that of the other species but the M−O stretches were shifted to higher energies due to the influence of the Ti atoms.

Solid State. The identities of the compound discussed above were determined by single-crystal X-ray diffraction investigations. Tables 1−3 list the data collection parameters for **1a**−**e**, **2**−**6**, and **8**−**12**, respectively. Full listing of the metrical data, thermal ellipsoid plots, and syntheses of **1**−**12** can be found in the Supporting Information. The consistency of the bulk powder with the observed structures was investigated by using solid-state NMR experiments. Table 4 lists the chemical shifts of the ^{13}C and ^{119}Sn MAS NMR spectra for these compounds.

Structures. While numerous arrangements were isolated for **1a**−**e** based upon the choice of crystallization solvent, the same basic subunit was found for each. The structure of **1** is the first THME-ligated Sn compound reported to date with the thermal ellipsoid plot shown in Figure 1 (structure shown is from **1c**). It is in a unique arrangement, consisting of three Sn atoms joined solely by the oxygens of the THME ligands. The THME ligands cap the Sn atoms above and below the plane of the metals forming a C_{3h} center of symmetry. Each Sn atom formally adopts a pyramidal (PYD) geometry; however, if the free electrons are included in the discussion, the geometry is best approximated by a square base pyramidal (SBP) geometry. Both arrangements force the electron pairs to reside externally.

Since there was very little difference in the metrical data between the individual species present in the crystal structures of **1** or between the various crystallized species (**1a**−**e**) only **1b** will be discussed. The Sn metal centers of **1b** are separated by an average of 3.46 Å with an average Sn−O distance of 2.20 Å. The $[-Sn-O]_2$ central cores possess very regular geometries with an average Sn−(μ-O)−Sn of 104.5 °, an average (μ-O)−Sn−(μ-O) from the same THME ligand of 78.7 °, and average (μ-O)−Sn−(μ-O) internal angle of 66.4 °. The shape of the molecule approximates an ellipsoid of ∼10 × 5 Å in size. The packing diagrams of **1a**−**e**, however, reveal that there is a great deal of flexibility in the arrangement of these subunits, the orientations of which are greatly dependent upon the solvent of crystallization.

Compound **2** (Figure 2) is a symmetric molecule consisting of a plane of four Sn cations in the trapezoidal arrangement. Two of the metal centers adopt a trigonal (TRI) and two adopt a PYD arrangement through the coordination of two THME and two NR_2 ligands. On each side of the plane of Sn atoms, each oxygen of the THME ligands is bound to each Sn metal center forming three $[-Sn-O-]_2$ moieties. The basal PYD-coordinated Sn cations are from THME oxygens only, whereas

Table 3. Data Collection Parameters for **8**−**12**

	8	9	10	11	12
chemical formula	$C_{24}H_{32}O_8Sn_4$	$C_{24}H_{32}O_8Sn_4$	$C_{26}H_{36}O_8Sn_4$	$C_{34}H_{52}O_8Sn_4$	$C_{30}H_{62}O_{10}Sn_3Ti$
formula weight	923.26	923.26	951.31	1063.52	986.77
temp (K)	168(2)	168(2)	168(2)	168(2)	168(2)
space group	*Pbca* orthorhombic	*Pbca* orthorhombic	*P*2(1)/*c* monoclinic	*Pbca* orthorhombic	*P*2(1)/*c* monoclinic
a (Å)	22.209(6)	20.967(4)	19.4460(14)	16.066(4)	17.174(10)
b (Å)	8.843(2)	8.9897(15)	8.3861(6)	17.328(4)	18.681(11)
c (Å)	29.053(8)	29.726(5)	18.4826(13)	28.081(6)	13.090(7)
β (deg)			92.6900(10)		106.920(10)
V (Å^3)	5706(3)	5603.1(16)	3010.7(4)	7818(3)	4018(4)
Z	8	8	4	8	4
D_{calcd} (Mg/m^3)	2.150	2.189	2.099	1.807	1.631
μ, (Mo Kα) (mm^{-1})	3.505	3.569	3.324	2.571	2.081
*R*1[a] (%)	3.16	3.56	3.31	3.84	7.25
*wR*2[b] (%)	6.66	6.53	5.76	5.93	12.76
*R*1[a] (all data, %)	4.77	5.76	6.81	9.09	19.98
*wR*2[b] (all data, %)	7.06	6.99	6.47	6.83	15.87

[a] $R1 = \sum||F_o| - |F_c||/\sum|F_o| \times 100$. [b] $wR2 = [\sum w(F_o^2 - F_c^2)^2/\sum(w|F_o|^2)^2]^{1/2} \times 100$.

Table 4. NMR Data for Selected Species

compd	^{119}Sn (THF-d_8)	119Sn MAS	^{13}C MAS
1	−330	−252	78.4 (OCH_2)$_3$CMe, 39.6 (OCH_2)$_3$*C*Me, 18.7 (OCH_2)$_3$C*Me*
2	+12, −331, −451	118, 94, −371, −382	78.6, 74.8, 73.8, 71.6, 70.5, 69.4 (OCH_2)$_3$CMe, 42.7, 42.3, 39.7 (OCH_2)$_3$*C*Me, 42.7, 42.3, 39.7 (OCH_2)$_3$*C*Me, 8.8, 7.2, 5.8 N(Si(*C*H$_3$)$_3$)$_2$
3	−330(1.25 Sn), −347(1.0 Sn), −372(2.0 Sn), −397(1.0 Sn).	−186, −208, −214, −230	75.7 ($CH_3C(CH_2O)_3$), 52.3, 51.4 (OCH_3), 41.8, 41.1 ($CH_3C(CH_2O)_3$), 20.5 ($CH_3C(CH_2O)_3$).
4	−330 (0.4 Sn), −351(1.0 Sn), −373 (2.1 Sn), −394 (1.0 Sn).	−190, −197, −213, −222	76.5, 75.6, 75.0 ($CH_3C(CH_2O)_3$), 57.0, 56.3 (OCH_2CH_3), 40.9 ($CH_3C(CH_2O)_3$), 21.9, 20.4 ($CH_3C(CH_2O)_3$), 18.9 (OCH_2CH_3)
5	−330(0.7 Sn), −366(1.0 Sn), −379(2.0 Sn), −391(1.0 Sn)	−203, −210, −218, −237	76.6, 74.8 ($CH_3C(CH_2O)_3$), 41.2, 39.2 ($CH_3C(CH_2O)_3$), 27.8, 19.6, 17.5, 16.1, 14.1 ($OCH_2C(CH_3)CH_2CH_3$, $CH_3C(CH_2O)_3$)
6	−330(0.7 Sn), −366(1.0 Sn), −377(2.0 Sn), −387(1.0 Sn)	−196, −241, −248	74.8, 74.5 ($CH_3C(CH_2O)_3$), 71.6, 70.9 (OCH_2CMe_3), 41.2. 40.5 ($CH_3C(CH_2O)_3$), 34.8 (OCH_2CMe_3), 30.7, 28.9 (OCH_2CMe_3), 20.1, 19.0 ($CH_3C(CH_2O)_3$).
7	−330(2.0 Sn), −390(1.0 Sn), −421(2.0 Sn), −464(1.0 Sn)	−126 (broad), −241, −280	159.9, 130.4, 123.0, 120.8 (OC_6H_5), 76.1, 74.8 ($CH_3C(CH_2O)_3$), 41.3 ($CH_3C(CH_2O)_3$), 21.0 ($CH_3C(CH_2O)_3$).
8	−330(0.25 Sn), −389(1.0 Sn), −420(2.0 Sn), −462(1.0 Sn)	−232, −242, −294	160.7, 159.6, 139.3, 131.9, 130.5, 122.6, 121.5, 120.8, 119.2 (OC_6H_4(Me)-3), 75.9, 74.3, 72.8 ($CH_3C(CH_2O)_3$), 41.7, 41.5 ($CH_3C(CH_2O)_3$), 23.3 (OC_6H_4(*Me*)-3), 20.6, 19.2 ($CH_3C(CH_2O)_3$)
10	−335(1.8 Sn), −372(1.0 Sn), −398(2.0 Sn), −417(1.0 Sn).	−220, −226, −257	130.8, 130.1, 129.4, 128.7, 125.8, 120.3, 119.3 ($OC_6H_3(Me)_2$-2,6), 77.4, 76.3, 74.6 ($CH_3C(CH_2O)_3$), 40.7, 40.1 ($CH_3C(CH_2O)_3$), 23.8, 23.1, 22.4 ($OC_6H_3(Me)_2$-2,6), 19.2, 18.4 ($CH_3C(CH_2O)_3$)
11	−208, −309, −339, −390, −403	-294, −324, −344, −361	155.6, 153.2, 142.7, 140.8, 138.9, 137.9, 125.8, 124.3, 118.6 ($OC_6H_3(CHMe_2)_2$-2,6), 76.1, 74.6, 73.1, 72.6 ($CH_3C(CH_2O)_3$), 56.2, 54.9, 49.3 ($OC_6H_3(CHMe_2)_2$-2,6), 40.3 ($CH_3C(CH_2O)_3$), 30.1, 29.7, 28.5, 27.8, 26.4, 25.6, 24.3 ($OC_6H_3(CHMe_2)_2$-2,6), 19.1, 18.3 ($CH_3C(CH_2O)_3$)
12	−358(1.0 Sn), −403(2.0 Sn)	−370, −403	83.7, 84.6, 85.5, 86.8 (OCH_2CMe_3), 79.7, 74.8, 76.5 ($CH_3C(CH_2O)_3$), 39.1, 38.5 ($CH_3C(CH_2O)_3$, 35.7, 35.3 34.8, 34.3($CH_3C(CH_2O)_3$), 29.7, 29.2, 28.8, 27.8 (OCH_2CMe_3), 19.0, 17.9($CH_3C(CH_2O)_3$)

the apical TRI-coordinated Sn atoms bind an NR_2 ligand to complete their coordination. The electrons of the apical Sn atoms point inward and the basal Sn atoms point outside from the molecule. The tridentate nature of the THME ligands forces the molecule into a cup shape that is open in comparison to **1**. In the literature, only two other crystallographically characterized Sn(OR)(NR_2) species have been reported, Sn(N(SiMe$_3$)$_2$)-($OC_6H_2(CMe_3)_2$-2,6,Me-4)[63] and [Sn(N(SiMe$_3$)$_2$)(μ-OBu)]$_2$.[64] The basal Sn atoms of **2** are separated by ∼3.43 Å wherein the apical Sn atoms are separated by ∼5.97 Å. The average Sn−N distances of 2.11 Å and the average Sn−OR distances of 2.20 Å are consistent with literature reports. The [−Sn−O]$_2$ central cores possess very regular geometries with Sn−(μ-O)−Sn that average 104.9 °, (μ-O)−Sn−(μ-O) that range from 67.6 to 121.5 °, and (μ-O)−Sn−N angles that average 92.8 Å. The distances of **2** are within agreement of those of the [Sn(N(SiMe$_3$)$_2$)(μ-OBu)]$_2$ dimer.[64]

Because of the similarity of the general constructs of **3**−**11**, the structures of these compounds will be discussed collectively. Each compound consists of a ring of four [−Sn−(μ-OR)$_2$−Sn] squares linked by Sn atoms. Six of the eight coordination sites of the four Sn cations are filled by the oxygen atoms of the THME ligands and two from the appropriate OR ligand. The

(63) Braunschweig, H.; Chorley, R. W.; Hitchcock, P. B.; Lappert, M. F. *J. Chem. Soc., Chem. Commun.* **1992**, 1311.

(64) McGeary, M. J.; Folting, K.; Caulton, K. G. *Inorg. Chem.* **1989**, *28*, 4051.

geometry around the metal centers approximates a SBP if the free electrons are included in the geometrical consideration. The OR ligands are bound to the same Sn atom and bridge to different Sn atoms in a trans arrangement. The remainder of the molecule consists of the bound THME ligands above and below the plane of Sn atoms. This results in one Sn atom with four μ-O_{THME}, two with three μ-O_{THME} and one μ-OR, and one with two μ-O_{THME} and two μ-OR oxygens atoms. The simplest mechanism for the formation of this arrangement is the side-on addition of the $Sn(OR)_s$ from the disruption of two Sn−O_{THME} bonds. The free electrons, as observed for **1**, are pointed externally for these molecule.

Metrical data of the alkoxide and aryloxide derivatives are all similar. The Sn- - -Sn distances were on average 3.55 Å for **3**−**6** and 3.57 Å for **8**−**11** which are substantially longer than those noted for **1**, reflecting the expansion of the original molecule. The Sn−(μ-THME) distances for the Sn−(μ-OR) and the Sn−(μ-OAr) species were ∼2.16 Å, independent of the OR group. The Sn−(μ-OR) distances systematically increase as the steric bulk around the metal center increases (av. 2.23 Å, **3**; 2.24 Å, **4**; 2.25 Å, **5**; 2.27 Å, **6**; 2.30 Å, **8**; 2.34 Å, **10**; 2.36 Å, **11**). The angles for the Sn−(μ-OR)−Sn range from ∼102.6 to 106.6 ° for **3**−**6** and ∼99.8 to 102.4 ° for **8**−**11**. In contrast, the Sn−(μ-THME)−Sn angles are much broader ranging, from ∼106.9 to 112.5 ° for **3**−**6** and ∼106.6 to 114.6 ° for **8**−**11**, due to the steric constraints invoked by the tridentate ligand.

For **12**, the central core resembles those of **3**−**11**. Observable by the presence of the hetero Ti atom, the μ-ONep ligands have rearranged and appear on the opposite side, *not* bound to the Ti metal center. Therefore, the assumption that simple expansion of the coordination sphere by a side-on addition noted for **3**−**11** is incorrect and a significant amount of ligand rearrangement must occur. The Ti uses four of the two THME ligands and two terminal ONep ligands to complete its octahedral geometry. Again the Sn atoms are PYD, using both THME and μ-ONep ligands. The Sn- - -Sn distance of **12** (av. 3.53 Å) is slightly shorter than what was noted for **3**−**11**, but the Sn- - -Ti distances are significantly shorter, at av. 3.44 Å. The Sn−O distances are within the range noted for **3**−**11** and the Ti−O distances are in agreement with the distances noted for [Ti(μ-ONep)-$(ONep)_3]_2$.[40] The angles around the Ti metal center are only slightly distorted from ideal octahedral angles. The geometry around the Sn cations is in agreement with those observed for **3**−**11**. On the basis of these data, the introduction of the Ti-$(OR)_4$ in comparison to the $Sn(OR)_2$ appears to have only subtly altered the basic constructs of the central core; therefore, it may be possible to add a wide range of metal alkoxides to yield a systematic method for production of mixed metal alkoxides.

Solid-State NMR. In an effort to verify that the bulk powders were consistent with the crystal structures, solid-state ^{13}C and ^{119}Sn MAS NMR investigations were undertaken. Crystalline material of each compound was packed into a rotor under an atmosphere of argon immediately prior to obtaining a spectrum. Table 4 lists the NMR data obtained on these compounds. The solid-state ^{119}Sn and ^{13}C MAS NMR spectra collected on the bulk powder of **1** are consistent with the symmetry observed for the single-crystal structures wherein a single ^{119}Sn MAS resonance and one set of THME ^{13}C resonances were observed.

The symmetry of **2** leads to two equivalent THME and $N(SiMe_3)_2$ ligands and two types of Sn metal centers. For the ^{13}C MAS NMR the representative ligand resonances are observed but are present as multiplets. The ^{119}Sn MAS NMR spectrum reveals four types of Sn metal centers: two around +105 ppm and two centered at −375 ppm. The ideal symmetry of **2** is disrupted in the solid state by intra- and interpacking inequivalancies. The four ^{119}Sn resonances may reflect the two types of Sn present (i.e., those bound by THME only ligands and those bound by THME and NR_2 ligands).

For **3**−**12**, each molecule possesses a C_2 axis of rotation which equates the THME and OR ligands and, therefore, one complete set of THME and OR ligand resonances is expected in the ^{13}C MAS NMR. The appropriate ^{13}C resonances are clearly present for each sample but many were duplicated, which can be attributed to many complications when looking at solid-state structures, including solid-state packing forces such as inequivalent pendant ligand groups, unit cell moieties (see Table 1−3), unit cell solvent inclusion, intermolecular generated packing inequivalancies, and/or asymmetry introduced by the OR groups which are not free to equilibrate in the solid state. Since an asymmetric molecule was observed in the ^{13}C MAS NMR, the ^{119}Sn MAS NMR should reveal four unique Sn peaks for **3**−**11** and three for **12**. The modification of **1** with an Sn-$(OR)_2$ or $Ti(OR)_4$ causes a significant change in the ^{119}Sn chemical shift as evidenced by a more than 100 ppm shift from **1** (see Table 4). For **3**−**5** and **11**, the expected four ^{119}Sn resonances were observed, but for **6** and **7**−**10**, three peaks were observed, each of which had a resonance around −240 ppm. For **12**, only two ^{119}Sn resonances were observed. The lower than expected number of ^{119}Sn MAS NMR peaks may be due to coincidental overlap of similar Sn environments. Considering the elemental analyses and infrared and solid-state NMR data *in toto*, the bulk powders of **1**−**12** appear to be consistent with the solid-state structure. It is of note that for every sample there was *no* ^{119}Sn peak observed that was consistent with compound **1** (i.e., compound **1** was not present).

Solution State. Due to the known dynamic behavior of metal alkoxides in solution, it was necessary to discern whether the solid-state structures of **1**−**12** were retained upon dissolution. Solution behaviors of **1**−**12** were investigated through the redissolution of crystals in THF-d_8. Samples were made as concentrated as possible without leaving any insoluble material in the NMR tubes, otherwise it is difficult to observe the ^{119}Sn signal.

The ^1H and ^{13}C NMR spectra of **1** in THF revealed three resonances consistent with the moieties of the THME ligand (methyl, quaternary, and methylene). A number of smaller peaks are present which are consistent with Sn- - -C *J*-coupling. The ^{119}Sn NMR spectrum indicates that the structure of **1** was retained in solution since only one peak was observed at δ −330 ppm. Therefore, the free electron pair on each Sn atom of **1** are still accessible in solution, which will allow for it to be used in a wide variety of applications, such as base catalyst (vide supra).

For each of the remaining samples (**2**−**12**), the ^1H and ^{13}C NMR spectra revealed multiple THME resonances and the respective OR or NR_2 resonances. These data were very complicated due to multiple overlapping resonances and did not significantly aid in interpretation of the solution behavior of the various compounds. In general, the ^{119}Sn NMR data were the most useful in clarifying the behavior of these compounds in solution.

The solid-state structure of **2** has two types of Sn atoms but the solution-state ^{119}Sn NMR spectrum revealed three peaks, one of which was consistent with compound **1** (δ −330 ppm). It has been reported that as the coordination number increases, the chemical shift is found further upfield.[65] Therefore, we assigned the upfield resonance (δ 451 ppm) to the 4-coordianted and the downfield resonance (δ +10) to the 3-coordinated Sn metal centers of **2**. Since the solid-state NMR data indicated that there was *no* **1** impurity present, this spectrum either must represent a decomposition of **2** in solution or an equilibrium must exist between **2** and its constituent parts (**1** and Sn(N(SiMe$_3$)$_2$)$_2$).

To verify this phenomenon, a sample of **2** was diluted, whereupon the ratio of the integration of the **1** to **2** resonances was increased. Variable-temperature NMR experiments revealed that at higher temperatures (>40 °C), the resonances associated with **2** increased in intensity. Combined these results suggest that for **2** the equilibrium discussed above exists (eq 3) in

$$(\mu\text{-THME})_2Sn_4(NR_2)_2 \xrightleftharpoons{THF} (\mu\text{-THME})_2Sn_3 + Sn(NR_2)_2 \quad (3)$$

solution. However, no signal for Sn(N(SiMe$_3$)$_2$)$_2$ (δ +766[63] in C_6D_6) was observed. A series of ^{119}Sn NMR spectra of Sn(N(SiMe$_3$)$_2$)$_2$ in THF-d_8 at different concentrations displayed a broad and weak signal that varied from δ −337 to −370 ppm. Therefore, the lack of a signal for Sn(N(SiMe$_3$)$_2$)$_2$ in the proposed equilibrium of **2** is most likely due to its weak signal and the small amount that would be generated. It is also of note that, over time, two additional peaks (δ −504 and +10 ppm) increased while the remaining resonances decreased, further demonstrating the unstable nature of **2** in solution.

Solution ^{119}Sn NMR data were also obtained for **3**−**11** and the expected 1:2:1 ratios of peak intensities were observed. However, for each sample, an additional signal at δ −330 ppm was observed, which is consistent with what was previously assigned to compound **1**. Compound **1** was not present in any of the solid-state MAS NMR spectra. Therefore, an equilibrium must exist as noted for **2** (eq 4), wherein **3**−**11** respectively are

$$(\mu\text{-THME})_2Sn_4(\mu\text{-OR})_2 \xrightleftharpoons{THF} (\mu\text{-THME})_2Sn_3 + Sn(OR)_2 \quad (4)$$

dissociated into **1** and the Sn(OR)$_2$. The absence of a ^{119}Sn signal for the Sn(OR)$_2$ is not surprising since these compounds lack a sharp ^{119}Sn signal and would only be present in a relatively small amount.

In an attempt to quantify the proposed equilibrium for **3**−**11**, the dilution of a select set of samples was followed by variable-temperature solution ^{119}Sn NMR. Dilution of a sample of **6** and **10** revealed a change in the ratio of the various peaks and variable-temperature NMR studies showed a broadening of the −330 ppm peak as the other peaks grew for both of these samples. This observation, and the fact that **1** was not observed in the solid state for any of these samples, indicates that an equilibrium as shown in eqs 3 or 4 must exist between these species in solution. The modification of **1** therefore is not as surprising as originally appeared since these molecules are fluctional in solution. The $^{117-119}$Sn ^2J-coupling normally associated with Sn−O−Sn linkages, and that typically range from 223[19,66] to 420−440[31,65,67] to 610 Hz,[65] was *not* observed for any of these compounds. This phenomenon was also previously reported for the similar $Sn_6O_4(OSiMe_3)_4$ compound[68] and attributed to rapid ligand exchange. The equilibrium (eq 4) described previously would account for the ligand scrambling and thus prevent the observation of the $^{117-119}$Sn ^2J-coupling.

For **12**, two ^{119}Sn resonances should be observed, but a significant shift should also be expected due to the presence of the Ti metal center and the sensitivity of the ^{119}Sn resonances to their environment. For **12** the chemical shift was shifted about 100 ppm further upfield in comparison to the other compounds. There is no indication of the δ −330 ppm peak and ^{117}Sn- - -^{119}Sn coupling was observed. This indicates that the structure of **12** is maintained upon dissolution. The presence of the Ti metal center with the increased Ti−O bond strengths and the octahedral geometry demanded by the Ti must reduce the ability to equilibrate. This stability would seem to favor the formation of other mixed-metal alkoxide complexes and these investigations are underway.

Applications

Due to the unique structures observed for these compounds in comparison to existing species, unusual properties are expected. For instance, based on the geometrical arrangement of **1** the free electron pairs on each of the metal centers point outward and are readily accessible. Since **1** was found to be relatively air stable and the solid-state structure was retained in solution, the utility of **1** as a base catalyst was investigated. A simple aldol condensation of acetaldehyde catalyzed by **1** revealed that greater than stoichiometric production of the expected condensation products occurs as determined by GC-MS experiments. Additional work to quantify this process with benzaldehyde to assist in quantification of the catalyzed product is currently underway.[47] The introduction of an alternative metal center into the framework of **1**, such as **12**, leads to the possibility of multiple catalytically active structurally rigid metal centers and/or single source MOCVD precursors.

Alternative to its catalytic nature, the DSC data for **1** indicated that this molecule may also be useful as a MOCVD precursor. Initial investigations of **1** with a simple vacuum MOCVD setup[69] revealed that high substrate temperatures are necessary for deposit (650 °C on a Pt/Si substrate), forming discrete uniform Sn° spheres (ranging from ~1 to 10 μm) instead of a SnO_x film.[47,70] The ease that **1** was modified, as evidenced by **2**−**11** (the properties of these compounds as MOCVD reagents) may be fine-tuned by introduction of alternative pendant ligands or altered to include other metals (i.e., **12**) for single-source reagents. Additional work in developing these MOCVD precursors is underway.

Summary and Conclusion

[Sn(N(SiMe$_3$)$_2$)$_2$]$_2$ was modified with the tridentate alkoxide THME-H_3 to yield a new family of compounds consisting of several unique shaped metal alkoxides (**1**, **3**− **11**), alkoxy amide

(65) Teff, D. J.; Minear, C. D.; Baxter, D. V.; Caulton, K. G. *Inorg. Chem.* **1998**, *37*, 2547.
(66) Lockhart, T. P.; Puff, H.; Schuh, W.; Reuter, H.; Mitchell, T. N. *J. Organomet. Chem.* **1989**, *366*, 61.
(67) Boegeat, D.; Jousseaume, B.; Toupance, T.; Campet, G.; Fournes, L. *Inorg. Chem.* **2000**, *39*, 3924.
(68) Sita, L. R.; Xi, R.; Yap, G. P. A.; Liable-Sands, L. M.; Rheingold, A. L. *J. Am. Chem. Soc.* **1997**, *119*, 756.
(69) Gallegos, J. J. I.; Ward, T. L.; Boyle, T. J.; Francisco, L. P.; Rodriguez, M. A. *Adv. Mater. CVD* **2000**, *6*, 21.
(70) Boyle, T. J.; De'Angeli, S. M.; Ward, T. L. Unpublished Results.

(**2**), and unique early main group mixed metal alkoxide species (**12**). Compound **1** appears by solid and solution state multinuclear (^{119}Sn, ^{13}C) NMR to maintain its solid-state structural arrangement in solution. Under relatively mild conditions, **1** can be easily manipulated to expand its central core, incorporating additional $Sn(OR)_2$ (**3**−**11**) or $Sn(NR_2)_2$ (**2**). In solution, for **2**−**11**, there appears to be an equilibrium between the solid-state structure and compound **1** and the parent alkoxides or amide. The exploitation of the expandability of **1** in both solution and the solid state was shown to exist for more than just $Sn(OR)_2$ through the introduction of a $[Ti(\mu\text{-ONep})(ONep)_3]_2$ forming **12**, which does not display dynamic behavior upon dissolution.

The introduction of the THME ligand has led to a versatile family of controlled structures that potentially have a wide range of applications. The transformation that **1** can undergo is well established in both the solid and solution state and is now being exploited as a stable scaffold to build larger more complex molecules. These tailor-made compounds will find utility in a variety of applications but currently are being explored as base catalyst and MOCVD processes. Further investigations into the chemistry and utility of this novel family of THME-ligated Sn precursors (**1**−**12**)[49] are currently underway.

Acknowledgment. For support of this research, the authors would like to thank the Office of Basic Energy Sciences of the Department of Energy and the United States Department of Energy under contract DE-AC04-94AL85000. Sandia is a multiprogram laboratory operated by Sandia Corporation, a Lockheed Martin Company, for the United States Department of Energy. The authors would also like to thank Dr. B. Cherry for his technical assistance in obtaining the ^{13}C and ^{119}Sn MAS spectra.

Supporting Information Available: X-ray crystallographic files (CIF) for the structures **1**−**12** and experimental details (PDF). This material is available free of charge via the Internet at http://pubs.acs.org.

JA0202309